SAND2016-1368C

The Derivation of Multiple-Input-Multiple Output (MIMO) Acoustic Test Specifications to Simulate a Missile Flight*

Jerome S. Cap
Sandia National Laboratories*
Program and Test Integration Department

Shantisa Norman
Sandia National Laboratories
Lightweight Structures Department

David O. Smallwood
Consultant

ABSTRACT

System level acoustic tests are often performed to simulate the environments associated with the powered flight phase of a missile flight. The traditional approach is to generate a uniform acoustic field around the structure. Some test setups attempt to tailor this uniform acoustic spectrum as a function of frequency to try and match a set of target acceleration responses on the structure. Such an approach is known as a Single Input Multiple Output or SIMO test. Sandia recently participated in a test series for which we derived a 12 source acoustic input designed to reproduce the flight data measured on 12 internal accelerometers on the structure for the lift-off phase of flight (i.e., a Multiple Input Multiple Output or MIMO test).

INTRODUCTION

While the goal of this acoustic test was to generate credible response data for structural locations that were not measured during flight, the focus of this paper will be to discuss the challenges associated with deriving a stable set of inputs for a MIMO acoustic test and show how well the flight responses were reproduced.

The authors of this paper would like to acknowledge the contributions of the Little Mountain Test Facility (LMTF) test team, who generated the necessary system identification data and implemented the recommended control strategies, and Ryan Shultz of Sandia, who performed Finite Element acoustic simulations that helped identify the means for reducing the error in the experimental acoustic model.

BACKGROUND

The purpose of this section is to describe the data formats, control strategy, test setup, and to discuss the decisions that had to be made to perform the tests.

For random vibroacoustic environments the tests are controlled in the frequency domain. Therefore, Auto Spectral Densities (ASDs) were used to characterize the flight and laboratory test responses. When the test called for using ASDs for multiple locations (inputs or responses) along with the corresponding phase and coherence information, a Spectral Density Matrix (SDM) was used. The diagonal terms in an SDM are the ASDs while the off-diagonal terms are the Cross Spectral Densities (CSDs), which contain the phase and coherence information. A valid SDM must be full rank (verified using the Matlab function ‘rank’) and positive definite (verified using the ‘p’ variable in the Matlab Cholesky factorization function ‘chol’).

While all of the computations and tests were performed using linear, narrowband spectra, it is considered best practice to present the results using 1/6th octave band frequency spectra. The use of $1/6^{th}$ octave bandwidth ASDs preserves the primary resonant character of the responses while reducing the variance error.

The first underlying assumption in this study is that the more response locations that the test can successfully reproduce, the more confidence one has in the responses measured at other locations. Table 1 identifies the available flight measurement locations.

* Sandia is a multiprogram laboratory operated by Sandia Corporation, a Lockheed Martin Company, for the United States Department of Energy under Contract DE-AC04-94AL85000

Table 1: Flight Instrumentation

Location	Axis	Location	Axis
A	X	D	X
	R		Y
B	X		Z
	R	E	X
C	X		Y
	R		Z

CONTROL STRATEGIES

How accurately a test reproduces the desired responses depends on how well the test setup replicates the boundary conditions during flight and the spatial variation in the acoustic excitation. Therefore, the second underlying assumption in this study is that a 12 input MIMO setup is better than a SIMO setup when trying to replicate multiple responses.

The Little Mountain Test Facility (LMTF), which performed the tests, uses a Spectral Dynamics Jaguar Multiple Input Multiple Output (MIMO) control system. This system is capable of independently controlling 12 banks of speakers. However, in order to conduct a MIMO test, one must define a set of inputs that replicate the desired responses, while meeting the requirement that the control SDM be positive definite and full rank. For the purposes of this test, the optimal test input was defined as the one that produced the best match for the flight spectra while minimizing the trace of the drive spectra.

TEST SETUP

Figure 1 shows the LMTF Direct Acoustic Field (DAF) test setup used for simulating the lift-off environment. This setup has 72 low frequency speakers grouped into 4 control zones and 72 mid-high speakers grouped into 8 control zones. A single Digital to Analog Converter (DAC) on the Jaguar system is dedicated to each zone.

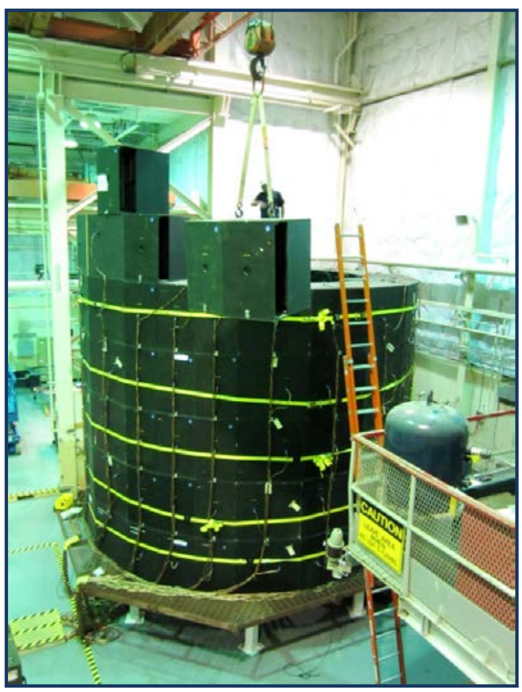

Figure 1: Little Mountain External Acoustic Test Setup

Figure 2 shows how the 12 speaker control zones are arranged around the unit. The 8 white rectangles represent the 8 independent high frequency zones (DAC channels 5-12), while the colored rectangles represent the 4 low frequency zones (DAC channels 1-4). The 180^o high-low configuration of the low frequency speaker banks was designed to provide the control system with the ability to produce both vertical and circumferential variation in the acoustic levels.

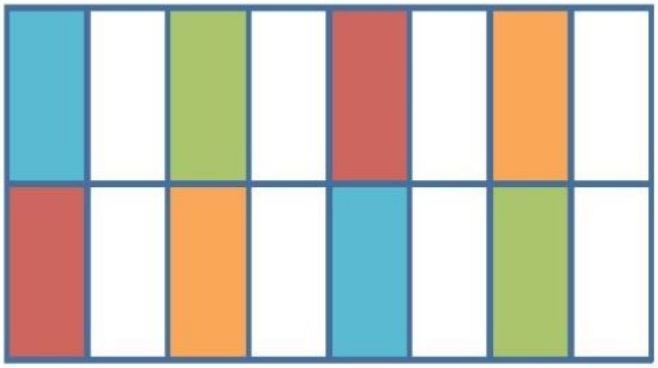

Figure 2: Little Mountain Control Zones (Unwrapped)

DEFINITION OF THE TRANSMISSIBILITY RESPONSE FUNCTIONS

Perhaps the most important experimental factor to making this analysis work is the measurement of good Transmissibility Response Functions (TRFs). A key requirement for achieving this goal is to insure that the inputs, S_{XX}, are independent (i.e., uncorrelated). At first glance the acoustic measurements would appear to be the best choice for the inputs, but they are highly correlated. Therefore, the decision was made to use the controller drive voltages as the “inputs” so the system was driven simultaneously using 12 uncorrelated DAC voltage inputs to generate the desired TRFs.

Earlier TRF measurements for related acoustic tests were flawed by the assumption that all that mattered when measuring TRFs was to keep the coherence between the inputs low and that meant having as many averages as possible so a 512 point block size (0.04 seconds long given a sample rate of 12800) with 50% overlap and a total of 1 minute of data were used for those analyses thereby generating 3000 blocks of data.

The resulting coherence between individual inputs, as defined by the off-diagonal terms in S_{XX}, was indeed small. However, the multiple coherence, M_{COH}, which quantifies the fraction of the total response that is related to the inputs [1], was also low. This meant that the TRF was not accounting for all of the energy and therefore would not be truly predictive of the input / output relationship.

By studying the FE model of the Little Mountain acoustic setup, it was shown that acoustic reflections were the main source of the incoherent energy. While the effect of reflections from earlier in time can never be completely eliminated, by using longer blocks of data for the TRF calculation the effects can be mitigated. Therefore, each block of data was defined to be 4096 points (0.32 seconds long), which allows for 18 reflections so any energy coming from an earlier block will be attenuated by 22dB by the end of the current time segment. This raised M_{COH} from ≈0.1-0.2 to ≈0.8-0.9 as seen in Figure 3 for a typical channel. The total record length was increased to 3 minutes to insure an adequate number of data blocks (using 50 % overlap 1124 data blocks were generated).

Using a longer block size would most likely have produced even higher M_{COH} values, but 4096 points per block was the longest block size compatible with the analysis of the flight data and it was desirous to keep the block sizes consistent between the flight and laboratory spectral analyses in order to avoid having to interpolate the TRFs (which can introduce error into the TRFs).

One key feature of the LMTF setup is that “crossover” filters are placed between the DACs and the amplifiers to prevent the control system from driving the amplifiers / speakers with out of band energy. Therefore, lowpass filters are applied to the drive voltages sent to the 4 banks of woofers and highpass filters are applied to the drive voltages sent to the 8 banks of mid/high speakers.

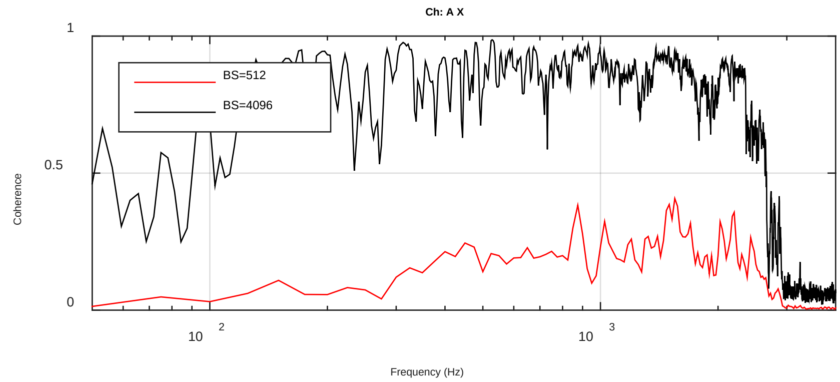

Figure 3: Multiple Coherence Examples

Figure 4 presents the TRFs between a typical lowpass (LF) and highpass (HF) filtered DAC input and a single accelerometer response channel. Figure 5 presents the same comparison for a typical control microphone. The accelerometer TRFs clearly show the effects of the crossover filters. For reasons that are not known to the authors, the effect is not evident in the microphone TRFs.

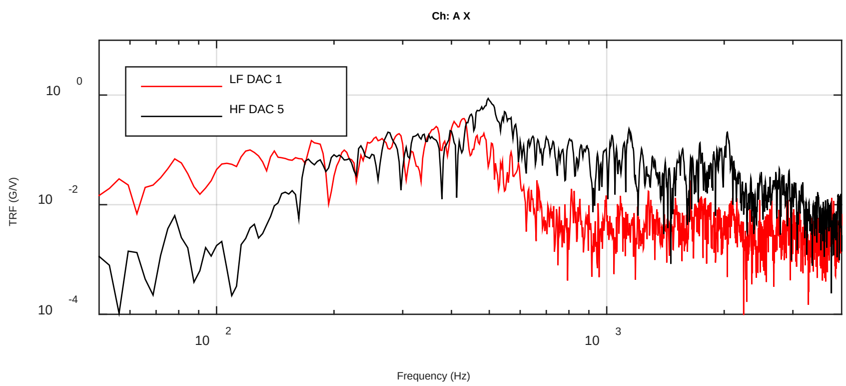

Figure 4: Drive Voltage to Response Acceleration TRFs

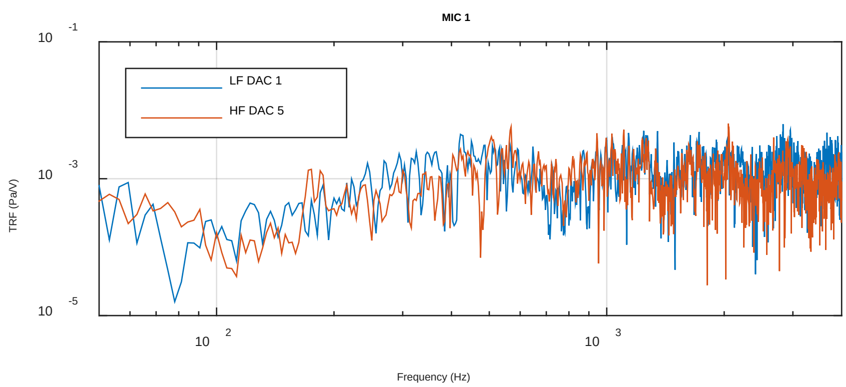

Figure 5: Drive Voltage to Microphone TRFs

DERIVATION OF INPUT SDMS

Conceptually the process of deriving the optimal inputs is straight forward. Equation (1) describes the relationship between the input SDM, S_{XX}, and the response SDM, S_{YY}, where H_{YX} is the Transmissibility Response Function (TRF).

$$S_{YY} = H_{YX} S_{XX} H'_{YX} \tag{1}$$

This equation is inverted to derive the optimal inputs as shown in equation (2).

$$S_{XX} = [H_{YX}^{-1}] S_{YY} [H_{YX}^{-1}]' \tag{2}$$

Since the drive voltages are being used as the "master inputs" the original plan was to derive the optimal drive voltages from the flight acceleration responses using equation (2) and then use equation (1) to generate the corresponding acoustic SDM for use in controlling the test with the microphones.

The appropriate algorithm for deriving the optimal input SDM depends largely on what we know about the response SDM. If one trusts that the phasing of the flight data was preserved and that the boundary conditions in the lab match the boundary conditions in flight, then one could use a Moore Penrose pseudo inverse (Matlab 'pinv') to derive the optimal input SDM. However, we could not verify that the phasing of the flight data was preserved, and perhaps more importantly we do not believe that the laboratory boundary conditions are the same as in flight.

Therefore, the decision was made to use David Smallwood's minimum drive algorithms [2, 3], which use two different techniques for generating the input SDM, having the minimum trace, that replicates the target response SDM. Both of Smallwood's algorithms allow the phase and coherence to be defined by the test setup. Appendix A presents a brief overview of Smallwood's algorithms.

PRACTICAL IMPLEMENTATION OF THE INPUT SDM

While in general the tests were successfully implemented, there were several practical issues that had to be addressed in order to generate an optimal, yet controllable input SDM.

The results produced by the minimum drive algorithms were just short of being a full rank, positive definite SDM (they were marginally unstable at a handful of frequencies). This is assumed to be at least partly due to the fact that the control scheme requires a rank 12 SDM, but the cross-over filters make the system look closer to rank 4 at low frequency and rank 8 at high frequency. Spectral Dynamic's recommended solution for such a situation is to scale the magnitude of the off-diagonal terms in the input SDM by 0.99. However, since scaling changes the input, Sandia chose to scale the results by a number as close to 1.0 as possible in increments of 0.001. The scale factor needed to make the initial estimate of the input SDM stable was 0.999.

Furthermore, the Jaguar control software does not preserve sufficient significant digits to handle a marginally stable input SDM. Therefore, additional scaling was needed. The supplemental scale factor needed to satisfy Jaguar was 0.997 so the net scaling was ≈0.996 (0.999*0.997).

The flight levels could not be achieved by the LMTF acoustic setup. The solution was simply to reduce the target levels until they could be achieved. The measured responses will be scaled by the corresponding scale factor to produce the estimated flight responses. The assumption is that the responses will scale linearly with the change in acoustic excitation levels. Response data measured for three acoustic levels (-12dB, -6dB, and 0dB) relative to the achievable response levels will be used to assess the linearity of the acoustic scaling.

The theoretical predictions of the responses based on the minimum drive analysis were very good with the exception of one narrow frequency band around 100 Hz. Unfortunately, the "as measured" responses were not as accurate. The possible root causes of this difference will be discussed later in this report. However, this fact made it necessary to have a metric by which to compare different test strategies. The formula in equation (3) was used to provide quantitative measure of how well a test performed.

$$E(dB) = 10\log(\frac{S_{YY(meas)}}{S_{YY(flt)}}) \quad (3)$$

The main source of error that could readily be corrected was the “bias error”. Bias error is essentially the mean of the channel specific errors as a function of frequency. Each term in the input SDM was scaled by the negative of the dB bias error and the test was repeated. This step succeeded in removing most of the bias error (it is assumed that the setup is just enough nonlinear so as to respond a little bit differently when subjected to the corrected inputs but this residual bias error was never deemed large enough to warrant a second correction).

As an aside, the inverse techniques used in this analysis employ a least squares error estimator based on the absolute error in the signals, which is slightly different than the formulation in equation (3) in that it will tend to optimize the highest magnitude responses at the expense of the lower magnitude responses. This is believed to be a contributor to the bias error. The fact that M_{COH} is less than 1 is also believed to contribute to the bias error.

As was mentioned earlier in this report, the original plan was to control the tests using the microphones even though the drive voltages were the true inputs. This was done based on concerns that controlling with the drive voltages might result in an “open loop” condition. However, while the Jaguar control system was adequately reproducing the desired acoustic SDM, it was observed that Jaguar was sending out of band energy to the speakers (i.e., high frequency energy to the woofers and low frequency energy to the mid/high speakers). This energy is subsequently filtered out by the crossover filters, but it was counting against the upper limit on the drive voltages, and thereby reducing the overall capacity of the acoustic system. In addition, the responses were not as good as the theoretical predictions.

Therefore, the decision was made to try and control the test using the drive voltage SDM. The results were better than expected.

1) The Jaguar stopped trying to send out of band energy to the speakers so we could achieve higher overall response levels (4dB higher for lift-off).
2) The dB error for the accelerometer responses became smaller.
3) The desired acoustic SDM was matched just as well as when the Jaguar was using the microphone SDM as the primary control target.

Figure 6 shows that both the DAC drive voltage and microphone controlled systems generally produce the desired acoustic levels. This shows that moving the control did not significantly alter the acoustic environment.

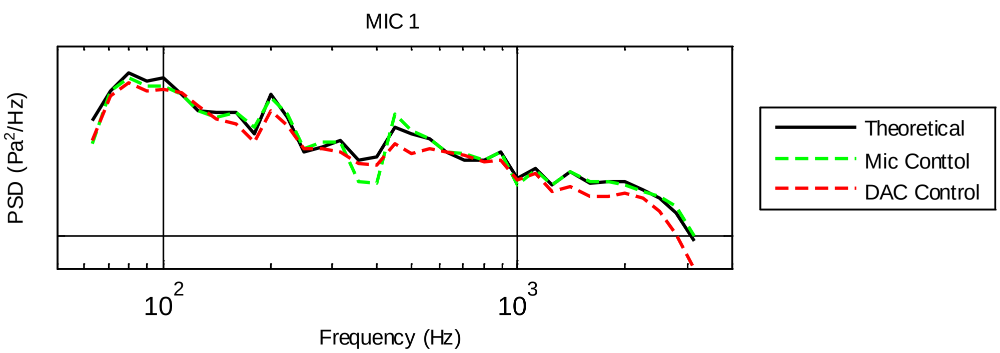

Figure 6: Microphone Pressures for MIMO Theoretical (Optimal) DAC, As Measured Microphone Control, As Measured DAC Control

However, the plots in Figure 7 show that while the DAC drive voltage control scheme closely replicates the predicted drive voltages (as one would expect), the microphone control scheme introduced high frequency input into the low frequency speakers even though this energy will be removed by the lowpass filters. The low frequency effects for the high frequency speakers are not as pronounced, but are still present.

Figure 8 presents the ensembles of dB errors for the theoretical optimum, the highest achievable level for the microphone control scheme (-28dB), and the highest achievable level for the drive voltage control scheme (-24dB). Because we switched from microphone control to DAC voltage control midway through the experiment, we did not perform a microphone controlled test with the bias error removed. Therefore, the reader should focus on the scatter in the data for the middle plot and not the mean error.

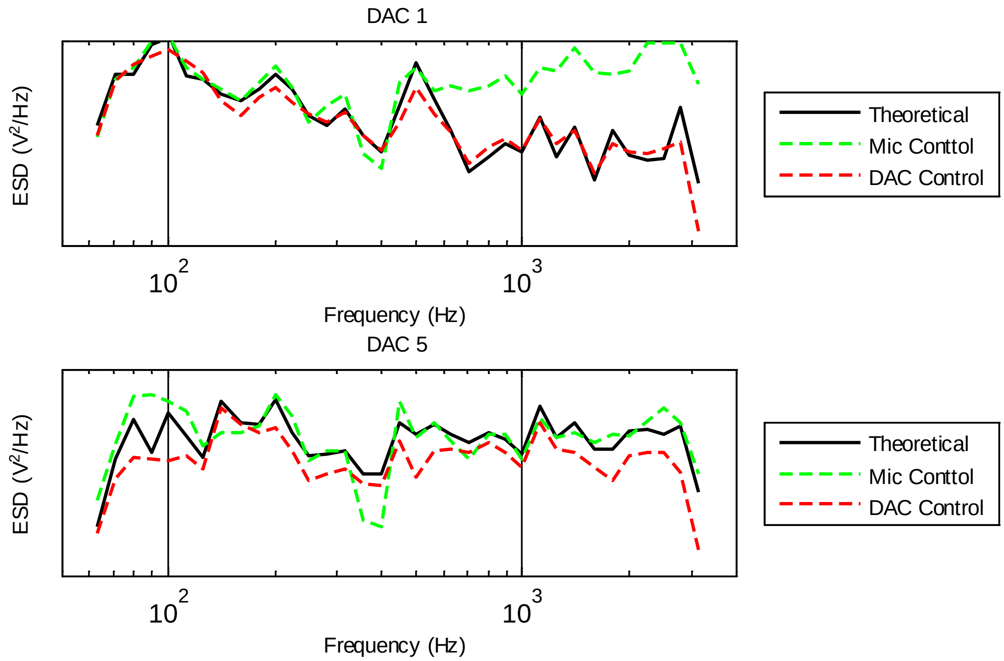

Figure 7: DAC Drive Voltages for MIMO Theoretical (Optimal) DAC, As Measured Microphone Control, As Measured DAC Control

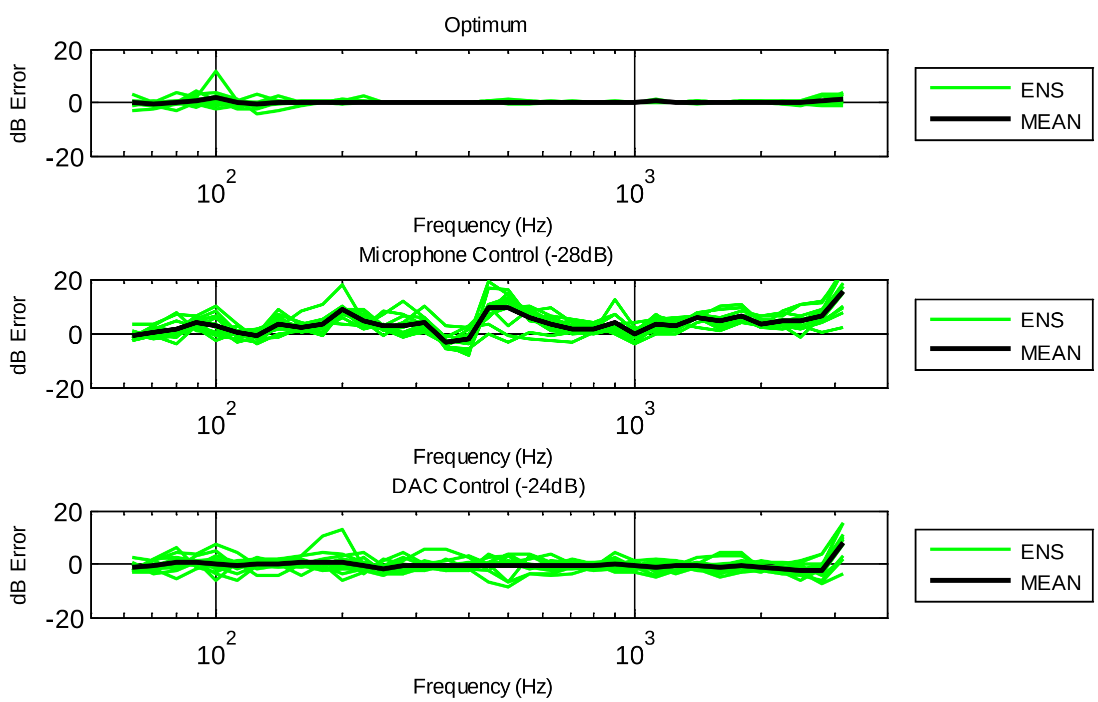

Figure 8: Error Ensembles for MIMO Theoretical (Optimal) Predictions and Two Alternate Control Schemes

Figure 9 presents the best achieved match for the 12 flight channels for lift-off corresponding to the bottom plot in Figure 8.

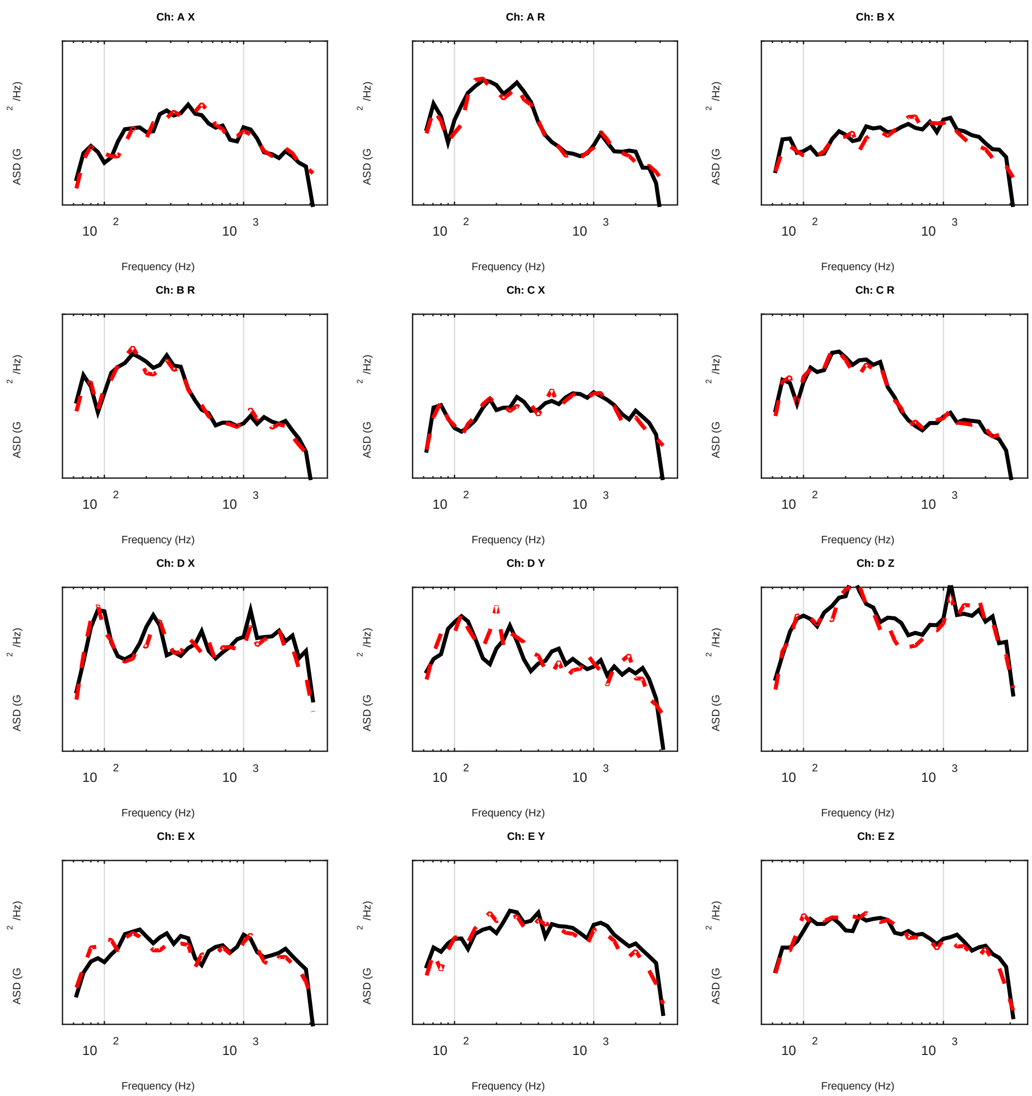

Figure 9: Best Effort MIMO Simulation (-24dB Re: Flight Responses)
Flight (Black), As Measured DAC MIMO Control (Red)

The absolute improvement in the target spectra associated with the DAC control scheme with respect to the microphone control scheme varied with frequency from virtually no change to significantly better. This combined with the fact that DAC control made it possible to achieve 4dB higher response levels was seen as justification to use the DAC control scheme.

As an aside, while we can't explain the connection, it is suspected that the issues associated with the "as generated" drive voltages not reflecting the effects of the cross-over filters when using microphone control might be linked to the fact that the microphone TRFs shown in Figure 5 do not exhibit the crossover effect (the JAGUAR can't account for something that isn't there). Conversely, it seems intuitive that linking the desired responses (the accelerometers) directly to the true input (the drive voltages) would make for the best results.

UNCERTAINTY ANALYSIS

Since the test results were not perfect, the logical next step was to perform an uncertainty analysis to better understand the source of the differences. There are two parts to the uncertainty analysis: 1) comparison of the MIMO results against the corresponding SIMO analysis, and 2) identification of potential sources of the observed error in the measured responses.

SIMO ANALYSIS

A lot of effort was put into deriving and implementing MIMO acoustic simulations. Therefore, it only made sense to establish the optimum SIMO simulation as a point of reference. The optimal SIMO inputs were generated analytically based on the assumption that a SIMO test would send a common drive voltage to each speaker bank.

Given this assumption, the first step was to create a SIMO TRF from the MIMO TRF. While the details are presented in Appendix B, each value in the SIMO TRF (size 12x1), H_{YXS}, is the sum of the terms in the corresponding row in the MIMO TRF.

The SIMO TRFs were used with the measured flight data, S_{YYF}, to generate an estimate of the optimal least squares input, S_{XXSO} using the inverse approach documented in [4]. The responses to this optimal input ASD, S_{YYSO}, as defined in equation (6), represent the best possible SIMO simulation for this test setup.

$$S_{YYSO(i)} = S_{XXSO}\left|H_{YXS(i)}\right|^2 \tag{6}$$

Figure 10 presents the optimal SIMO responses. Since the main errors associated with the MIMO simulations were experimental in nature, the decision was made to compare the optimal theoretical SIMO results against the optimal theoretical MIMO results in order to have an apples-to-apples comparison (i.e., it is assumed that the SIMO errors presented here will get somewhat larger if a SIMO test were actually conducted). Therefore, Figure 11 compares the optimum theoretical SIMO and MIMO dB errors.

The optimal SIMO responses were generally 5-10 dB worse than the corresponding MIMO responses. Whether or not this error would translate to an actual test is not known (while some sources of error apply to both control schemes, the SIMO system might actually be a little easier to control).

IDENTIFICATION OF ERROR SOURCES

Since the actual results did not match the theoretical results, the decision was made to investigate possible sources of error that could be eliminated or reduced for future testing. Three possible sources of error were identified:

1) Inaccuracy in the TRFs due to the reverberation in the chamber.
2) Inability of the control system to conduct a perfect test.
3) The scaling of the off-diagonal terms used to keep the control system stable.

Based on the discussion earlier in this paper regarding the accuracy of the TRFs, it is assumed that any issue associated with the TRFs will primarily manifest itself as an offset in the mean response (i.e., a bias error) and not as an increase in the variance in the responses. Therefore, this section will focus on the latter two potential sources of error.

It is accepted that one can never control the test perfectly but it is assumed that controlling a MIMO test is more difficult than controlling a SIMO test. Therefore, it is reasonable to assume that differences between the desired and achieved drive voltages could be a significant source of error. Therefore, the DAC control error was computed using equation (3) with the ratio of the measured DAC voltage SDM divided by the optimal input DAC voltage SDM (the red and black lines respectively in Figure 7 are examples of these values).

At first glance one might think that scaling the off-diagonal terms in the input SDM by 0.997 would not represent a significant change. However, depending on the relative contribution of the 12 inputs to a given response, this translated into a 3% error. The input SDM off-diagonal scaling error was computed using equation (3) with the ratio of the theoretical accelerometer responses generated using the optimal input SDM scaled by 0.999 (the minimum scale factor needed to insure a full rank positive definite SDM) and the same input SDM scaled by 0.996 (the as-tested scaled SDM). Hence, the resulting dB error reflects the effect of reducing the off-diagonal terms by 0.997.

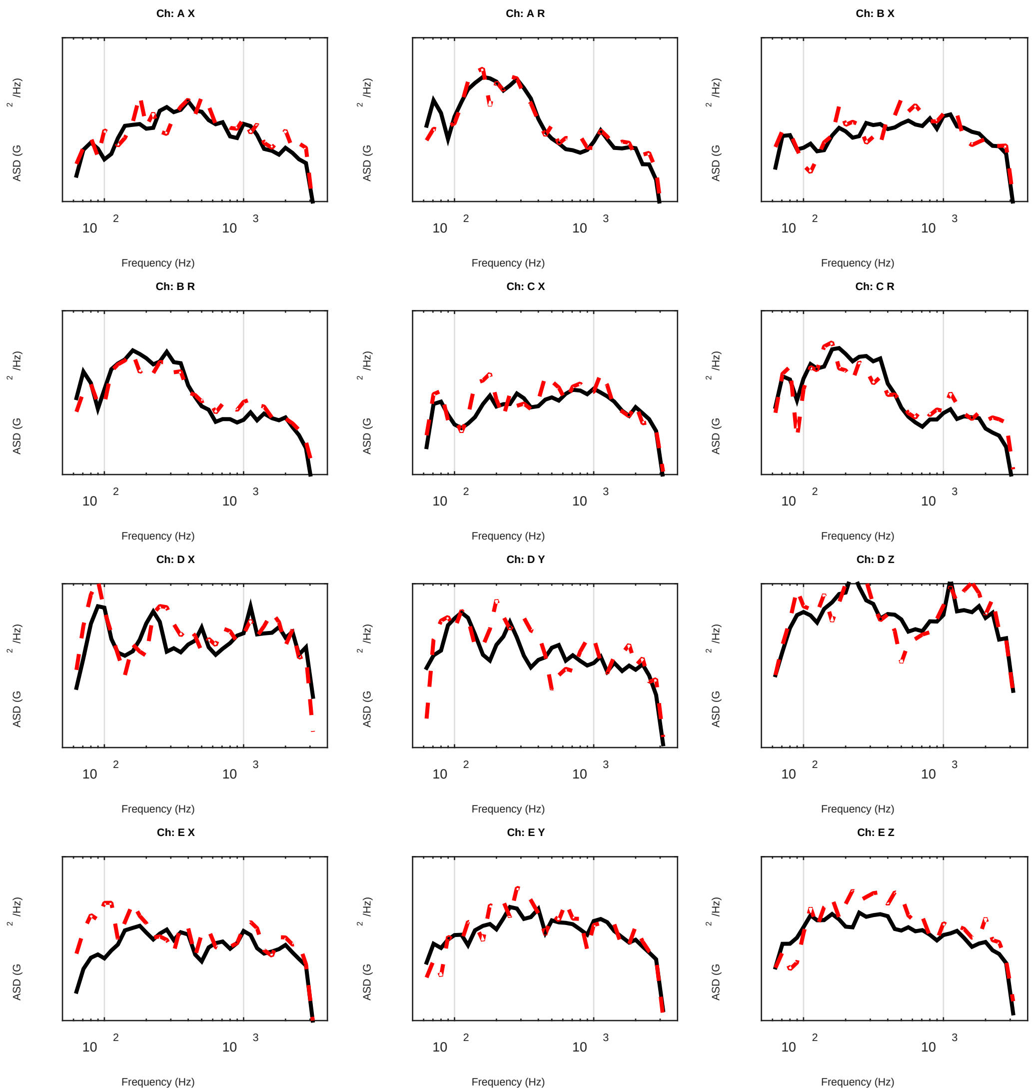

Figure 10: Best Effort SIMO Lift-off Simulation (-24dB (Re: Flight Responses)
Flight (Black), Theoretical SIMO (Red)

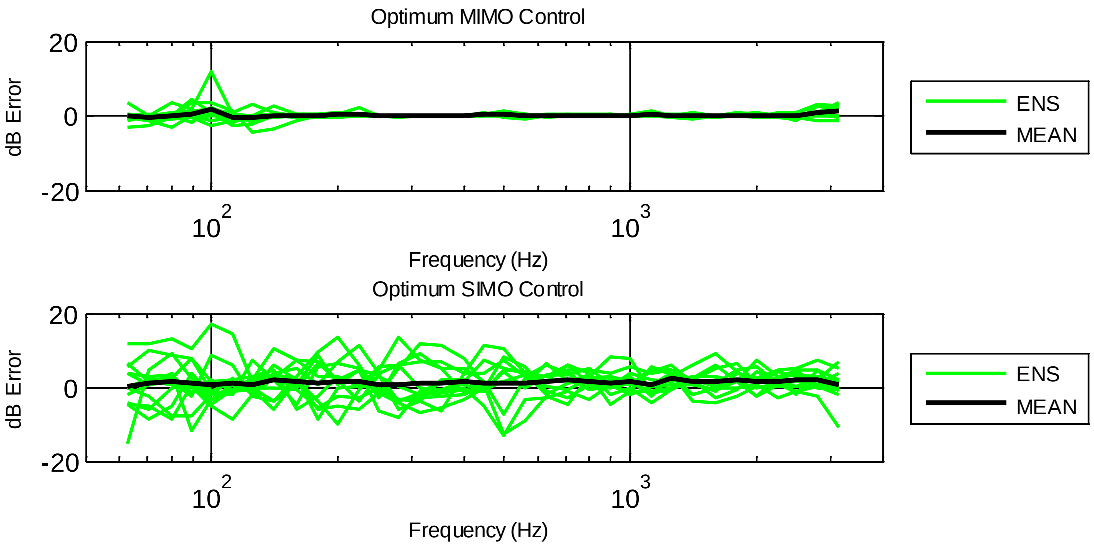

Figure 11: Error Ensembles for Optimum Theoretical MIMO and SIMO Lift-off Simulations

The top plot in Figure 12 presents the total "as measured" dB error ensembles for the final best effort MIMO simulation (same as the top plot in Figure 6). The middle and bottom plots in Figure 12 present the DAC control error and the off-diagonal scaling error respectively. The bias error has been removed from these ensembles so that the reader can focus on the variation.

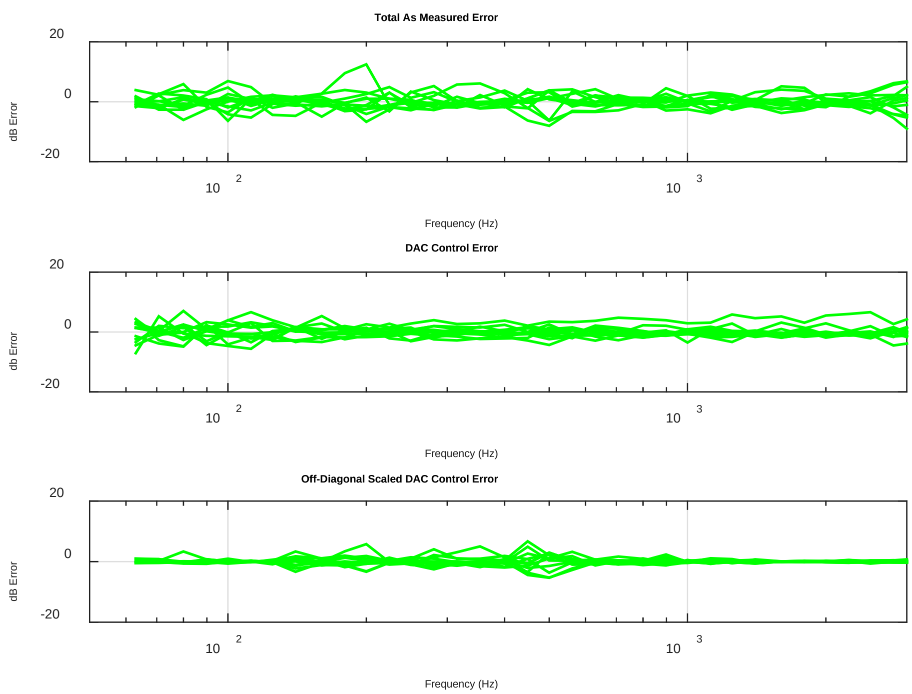

Figure 12: Comparison of Control System Error and Off-Diagonal Scaling Errors versus Overall Error

While no attempt was made to correlate these errors, there is certainly enough error associated with the DAC control and the off-diagonal scaling to account for much of the error in the measured responses. Since these sources of error are closely linked to the control system, it is assumed that we would expect to see similar results for any future testing conducted in the same manner.

SUMMARY AND CONCLUSIONS

While some aspects of the input derivation and test setup could have been done better, since an accurate simulation of the target flight responses was achieved the overall results of this test series were considered to be very good.

The fact that the analytical MIMO simulations produced better results than the corresponding SIMO simulations would appear to justify the decision to go with the more complicated testing approach.

Follow-on efforts include the scaling of the responses to flight levels and interpretation of the errors for response channels other than the flight channels.

APPENDIX A: MINDRIVE TIKHONOV REGULARIZATION ALGORITHMS

As was stated in the main section of this document, the decision was made to not use the phase and coherence information from the flight data. Therefore, two methods, both of which rely only on the magnitude of the flight ASDs, were implemented for this project: 1) an independent drive algorithm [3], and 2) an Eigenvalue Decomposition algorithm [4]. The method producing the minimum trace of the input SDM was used to define the test input.

INDEPENDENT DRIVE ALGORITHM

For this approach, a set of independent drives, S_{XXI}, (i.e., the off-diagonal terms are set to zero) is convolved with the system TRFs, H_{YX}, to produce a set of responses, S_{YYI}, as shown in equation (4).

$$S_{YYI} = H_{YX} S_{XXI} H'_{YX} \tag{4}$$

S_{YYI} is then rescaled so that the diagonal terms match the corresponding terms in the target SDM, S_{YY}, while preserving the phase and coherence of S_{YYI}. This is accomplished by dividing the individual terms, $S_{YYI}(IJ)$, by the square root of the product of the 'ith' and 'jth' diagonal terms and then multiplying by square root of the product of the 'ith' and 'jth' flight ASDs. The resulting SDM is identified as S_{YYIC}.

The input SDM that will produce the rescaled response SDM, S_{XXIC}, is computed using the Moore Penrose pseudo inverse with Tikhonov regularization as shown in equation (5).

$$S_{XXIC} = [H_{YX}^{-1}] S_{YYIC} [H_{YX}^{-1}]' \tag{5}$$

S_{XXIC} is no longer truly independent but this approach is generally stable. The reader should note that this approach assumes that the best estimate of the phase and coherence are whatever naturally exists in the test setup when excited by independent drives. How well the test setup and the assumption of independent drives approximate the field configuration is presumably the deciding factor in determining the realism of these inputs.

EIGENVALUE DECOMPOSITION ALGORITHM

For this approach the goal is to define the response SDM, S_{YYC}, that when multiplied by the inverse of the TRF, H_{YX}, as shown in equation (6) will produce the minimum trace input SDM, S_{XXC}.

$$S_{XXC} = [H_{YX}^{-1}] S_{YYC} [H_{YX}^{-1}]' \tag{6}$$

Where the inverse of H_{YX} is computed using the Moore Penrose pseudo inverse (Matlab function pinv).

In order to accomplish this goal, the diagonal terms in S_{YYC} are set equal to the flight ASDs, while the off-diagonal terms in S_{YYC} are defined so as to produce the minimum trace. However, this matrix is not always positive definite. Therefore, an Eigenvalue Decomposition is performed on this response SDM per equation (7) where *D* contains the eigenvalues and *V* contains the eigenvectors.

$$S_{YYC} = V^*D^*V' \tag{7}$$

Each negative eigenvalue, *D(i)*, is replaced with a small positive value, $D_0(i)$. The corrected response SDM, S_{YYC0}, is then reconstructed using equation (8).

$$S_{YYC0} = V^*D_0{}^*V' \tag{8}$$

This approach will produce the minimum input SDM if the corrections are small.

APPENDIX B: DERIVATION OF SIMO TRFs

The transformation from a MIMO TRF to a SIMO TRF is based on the underlying definition of the TRF as shown in equation (9) where *X* is the 12x1 vector of inputs, *Y(j)* is the 'jth' response, and $H_{YX}(j,i)$ is the 'ith' column in the 'jth' row in the MIMO TRF.

$$\{Y(j)\} = \sum_{i=1,12}[H_{YX}(j,i)]\{X(i)\} \tag{9}$$

If one defines all 12 values in *X* to be identical (i.e., $X=X_S$), then equation (4) can be rewritten as shown in equation (10).

$$\{Y(j)\} = X_S \sum_{i=1,12}[H_{YX}(j,i)] \tag{10}$$

Hence, each value in the SIMO TRF (size 12x1), H_{YXS}, is the sum of the terms in the corresponding row in the MIMO TRF.

REFERENCES

[1] David O. Smallwood, "Matrix Methods for Estimation the Coherence Functions from Estimates of the Cross-Spectral Density Matrix", Shock and Vibration, Vol. 3, No. 4, p. 237-246 (1996).

[2] David O. Smallwood, "A Proposed Method to Generate a Spectral Density Matrix for a Multiple Input, Multiple Output Vibration Test", Proceedings of the 81st Shock & Vibration Symposium, Oct 2010, Orlando FL.

[3] David O. Smallwood, "A Revised Algorithm for Minimum Input Trace to a Multiple-Input / Multiple-Output system (MIMO) to Match the Output Autospectral Densities", Proceedings of the 85st Shock & Vibration Symposium, Oct 2014, Reston, VA

[4] Jerome S. Cap, Melissa K. C' de Baca, and David O. Smallwood, "A Technique for the Identification of the Optimum Inputs for a Vibration or Acoustic Test"; Proceedings of the 76th Shock & Vibration Symposium; October 31st – November 3rd, 2005; Destin, FL.